Department of Mechanical Engineering

National Institute of Technology Rourkela

VIBRATION ENERGY HARVESTING FROM A PIEZOELECTRIC CANTILEVER BEAM

Thesis submitted in the partial fulfillment

of the requirements for the degree of

Bachelors of Technology

in

Mechanical Engineering

by

Moses Prasad Varghese

(Roll Number: 114ME0039)

based on the research carried out

under the supervision of

Professor R.K. Behera

May 2018

Department of Mechanical Engineering

National Institute of Technology Rourkela

VIBRATION ENERGY HARVESTING FROM A PIEZOELECTRIC CANTILEVER BEAM

Thesis submitted in the partial fulfillment

of the requirements for the degree of

Bachelors of Technology

in

Mechanical Engineering

by

Moses Prasad Varghese

(Roll Number: 114ME0039)

based on the research carried out

under the supervision of

Professor R.K. Behera

May 2018

Department of Mechanical Engineering

National Institute of Technology Rourkela

May 2018

Certificate of Examination

Name: Moses Prasad Varghese

Roll number: 114ME0039

Title of thesis: Vibration energy harvesting from a piezoelectric cantilever beam

I the below signed, after checking the dissertation mentioned and the official record book(s) of the student, hereby state the approval of the thesis submitted in partial fulfillment of the requirements for the degree of *Bachelors of Technology* in *Mechanical Engineering* at *National Institute of Technology Rourkela*. I am satisfied with the volume, quality, correctness and originality of the work.

Department of Mechanical Engineering

National Institute of Technology Rourkela

May 2018

Supervisors' Certificate

This is to certify that the work presented in the thesis entitled "*Vibration energy harvesting from a piezoelectric cantilever beam*" submitted by *Moses Prasad Varghese- 114ME0039*, is a record of original research carried out under my supervision and guidance in partial fulfillment of the requirements for the degree of *Bachelors of Technology* in *Mechanical Engineering*. Neither this thesis nor any part of it has been submitted earlier for any degree or diploma to any institute or university in India or abroad.

R.K. Behera
15/05/2018

R.K. Behera

(Professor)

Declaration of Originality

I hereby declare that this thesis entitled "*Vibration energy harvesting from a piezoelectric cantilever beam*" presents my original work carried out as a Bachelor student of NIT Rourkela and, to the best of my knowledge, contains no material previously published or written by another person, nor any material presented by me for the award of any degree or diploma of NIT Rourkela or any other institution. Any contribution made to this thesis research by others, with whom I have worked at NIT Rourkela or elsewhere, is explicitly acknowledged in the thesis. Works of other authors cited in this dissertation duly acknowledged under the sections References or Bibliography. I have also submitted the original research records to the scrutiny committee for evaluation of my dissertation.

I am fully aware that in case of any non-compliance detected in the future, the Senate of NIT Rourkela may withdraw the degree awarded to me on the basis of the present thesis.

May 2018 Moses Prasad Varghese

NIT Rourkela

Acknowledgment

May 2018 Moses Prasad Varghese

NIT Rourkela

I am profoundly obligated to my project guide Dr. R. K. Behera for giving me the opportunity to take up this project under his capable guidance. He has been an extraordinary mentor and had provided me with the motivation required throughout the year. I am appreciative of him for being so patient with me and for providing me with the necessary tools, information to successfully complete the project.

I am also grateful to every one of the instructors and staffs of the Department of Mechanical Engineering for continually being accessible to me in clearing some questions or different issues which were impeding my advancement in my project work.

Finally, I would like to thank my Almighty for giving me such magnificent guardians and kin and for investing me with the essential abilities to overcome all chances and emerge triumphantly.

Abstract

Vibration energy harvesting is a method for converting mechanical energy from different ambient sources to electricity in the form of electric voltage. Many researchers have developed linear resonators which have poor performance in areas far from the natural frequency. So here we investigate a nonlinear vibration energy harvester which has not the only advantage of broader frequency spectrum but also higher amplitude. In order to achieve this objective, a system which combines both bi-stability and internal resonance is presented. The system consists of a piezoelectric cantilever beam with a movable magnet at the free end facing a fixed magnet. A spring is attached to the beam which allows the magnet to move along the beam which further increases the amplitude of the vibration. To obtain dynamic response of the beam, movable magnet and the output voltage extended Hamilton's principle and Galerkin decomposition method is used to obtain governing equation of motion. The method of multiple scales (MMS) is used to solve the governing equations in order to obtain approximate analytical solution and the frequency response was obtained for amplitude and output voltage. The effect of different system parameters on the frequency response was also analyzed.

Keywords: Nonlinear vibration, Energy harvesting, Internal resonance, Bi-stability

Contents

List of Figures

List of Tables

Chapter 1

INTRODUCTION

Energy harvesting is a technology that has increasing demand for sensors and microsystems. Mechanical vibration is one among the sources of energy which can be converted to the electrical voltage. This source of energy can substitute batteries and alternative short life energy storage system that have high maintenance cost as given by Wei Yang et al. [1]. The current researchers primarily specialize in linear systems that have restricted frequency bandwidth that limits the efficiency of the system because it causes decrease in the output once the excitation frequency differs from the resonant frequency as shown by S.P. Pellegrini et al. [2]. The reason that ambient mechanical vibration has large frequency spectrum or bandwidth, result in the analysis of nonlinear systems. Some of the methods we're using stoppers for analyzing the spring hardening impact as shown by H. Liu et al. [3], using preload that is axial and static to increase the stiffness of the structure as shown by R. Masana et al. [4] and application of parametric excitation. Yildirim et al. [5] recently designed a clamped-clamped beam with a movable central magnet within a coil. The experiment showed frequency softening and a broader bandwidth near the first and principal parametric resonances. Nonlinearity from bi-stable systems can also broaden the frequency bandwidth. Such systems use two magnets (one stationary and one moving) for piezoelectric energy harvesters as analyzed by F. Cottone et al. [6] to make a double-well potential function. Their performance was studied beneath base vibrations of harmonic and random natures as shown by B. Ando et al. [7]. Across numerous excitation levels, bi-stable systems outperformed linear ones. Bi-stable systems conjointly were utilized in electromagnetic generators as analyzed by B. Mann et al. [8] and Y. Chen et al. [9].

The magnetic force adds cubic stiffness nonlinearity and makes the oscillator a Duffing kind with frequency hardening behavior as shown by B. Mann et al. [8] and D.A. Barton et al. [10]. Daqaq [11] investigated the response of such harvesters as a unimodal Duffing-type oscillator exposed to White Gaussian and Colored excitation. Zou et al. [12] proposed a compressive-mode wideband vibration energy harvester employing a combination of bistable and flextensional mechanisms. Most vibration energy harvesters use one degree-of-freedom system. However, to extend the frequency bandwidth, many multi-degree-of-freedom approaches have been proposed. Wu et al. [13] reported that a two degrees-of-freedom harvester can achieve two close resonant frequencies with significant power outputs by using two cantilever beams with magnetic tips. Tang et al. [14] proposed a piezoelectric harvester composed of a cantilever with a magnetic tip facing a movable magnet, replacing the fastened magnet in typical bi-stable harvesters. The power output had large amplitude over a broad bandwidth. Using two orthogonal cantilever beams with magnetic tips, Ando et al. [15] bestowed a coupled bi-stable system that showed high outputs at low frequencies for bi-directional vibrations. Increasing degrees of freedom by adding multiple wound cantilever beams nearby a fixed magnet was conjointly investigated by Sari et al. [16] that showed increase of the frequency bandwidth for micro electromagnetic generators. Internal resonance is another nonlinear phenomenon that may be used to broaden the bandwidth as shown by A. Nayfeh et al. [17]. Amplitude frequency responses of internal resonators bend to two opposite frequency directions inflicting a rise in the frequency bandwidth for energy harvesting. Lan et al. [18] analyzed the energy harvesting of a vertical piezoelectric beam with its mass at the tip beneath vertical excitations. Static and dynamic instabilities were used to produce large amplitudes. Strong internal resonance of the system improved energy conversion efficiency under harmonic and random excitations. Chen and Jiang [19] showed that energy

harvesting based on internal resonance produced more power in comparison to a linear system by the use of mechanical oscillator to an electromagnetic energy harvester. Using an L-shaped piezoelectric structure with quadratic nonlinearity, Cao et al. [20] showed exploitation of its two-to-one internal resonance increased significant frequency bandwidth compared to its 2-DOF counterpart. This increase was achieved for excitation frequencies close to the primary and second linear natural frequencies. Additionally to an L-shaped piezoelectric beam, Chen et al. [21] used magnets to enhance the performance by increasing the bandwidth of energy harvesting. By changing the gap between two magnets, the harvester can put in internal resonance to widen the frequency bandwidth and increase output. The contributions of this thesis is to combine bi-stability and internal resonance effects to broaden the frequency bandwidth of nonlinear vibration energy harvesting. This is achieved by using a system that consists of a cantilever beam with tip magnet facing a fixed magnet. Bi-stability is introduced by the magnetic interactions, whereas the movable magnet generates internal resonance. Bi-stability can broaden the frequency bandwidth, however the increase isn't substantial. Combining the two effects leads to a larger frequency bandwidth that can increase energy conversion efficiency. In this thesis, we tend to add a piezoelectric strip to the beam for energy harvesting and develop an electromechanical coupled mathematical model of the system. The content of this thesis is organized as follows. Chapter two describes a mathematical modeling of the combined resonator followed by the perturbation method of multiple scales to solve for the steady-state frequency response. A linearized piezoelectric coupling was used to simulate the electromechanical performance. The obtained solutions are described in chapter three. The effects of various system parameters on the electromechanical frequency responses are investigated in chapter four. Chapter five concludes the thesis.

Chapter 2

METHODOLOGY ADOPTED

The energy harvester consists of a piezoelectric cantilever beam with a movable magnet connected to a spring and another fixed magnet with the arrangement of repulsive magnetic force that's shown in Figure 1. The cantilever beam is totally covered by the piezoelectric material and the spring on the beam permits the movable magnet to slide along the beam. The entire structure is connected to a parent host that generates a mechanical vibration in the horizontal plane allowing the beam to vibrate within the same plane. Our goal is to increase the vibration amplitude of the cantilever beam to maximize the piezoelectric voltage output. This goal is achieved using the movable magnet and the working principle is explained in the next section.

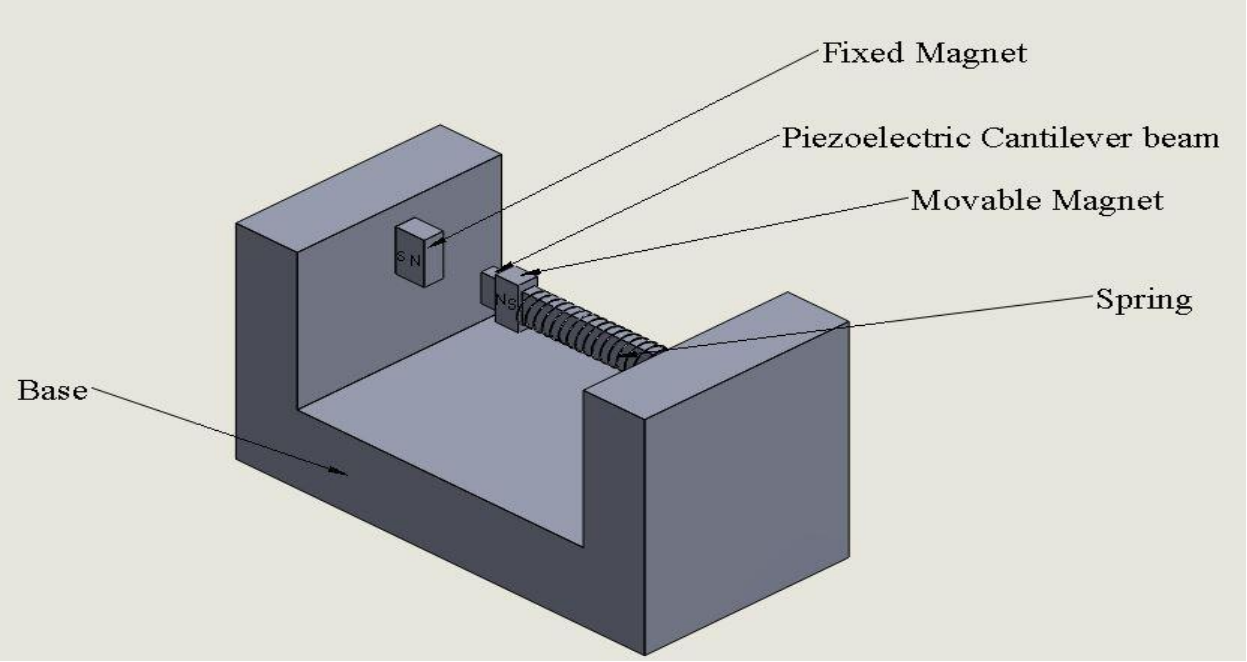

Figure 1: Vibration energy harvester model

2.1 Working Principle

The initial position of beam and magnets are shown in Figure 1. The vibration of the base perpendicular to the beam length causes two terminal positions of the beam in the horizontal plane. At the initial, centered, position of the beam, the tangential component of the magnetic force compresses the spring. As the beam vibrates away from the middle position, the impact of the tangential component wanes while the normal component becomes stronger. The reduction in the tangential component makes the spring stretch, reducing the horizontal distance between the magnets. The normal component of the magnetic force increases with this distance reduction, hence bending the beam to its largest displacement. At this terminal position, the restoring force of the beam overcomes the normal magnetic force and the beam vibration reverses causing the spring to compress again. The increase in the beam displacement caused by the increase of the normal magnetic force is exclusive for this movable magnet configuration. The larger the displacement, larger the piezoelectric output voltage.

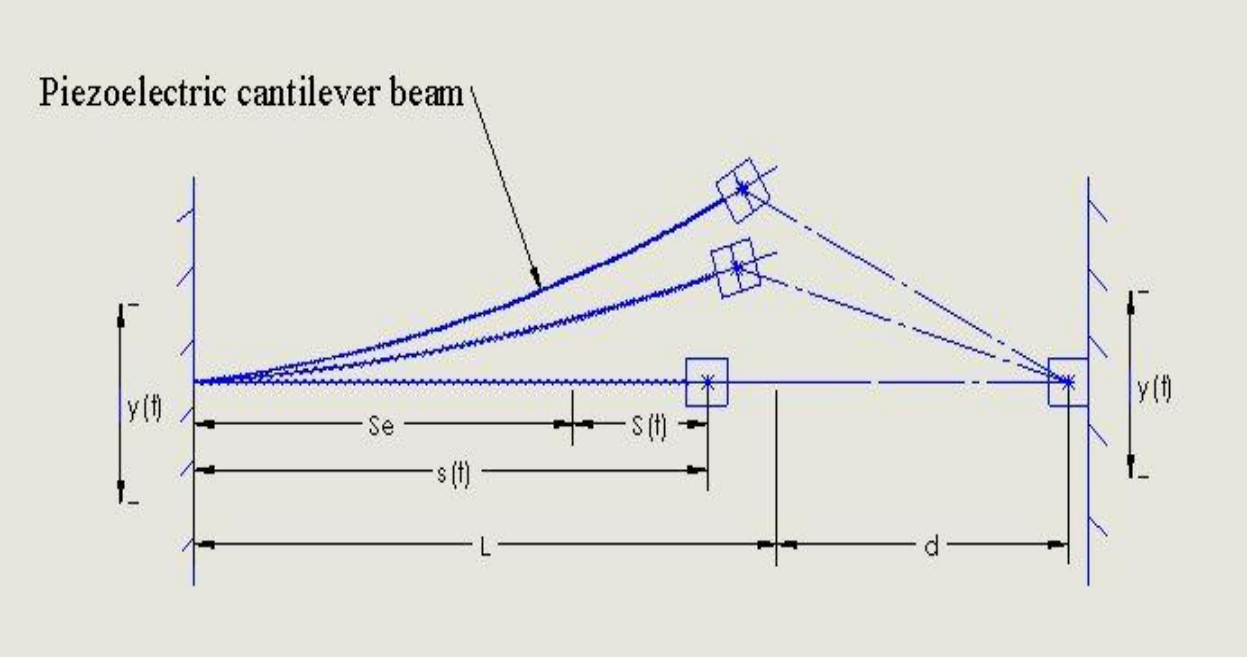

Figure 2: Beam with movable and fixed magnet

In Figure 2, s(t) is the position of the movable magnet measured from the fixed support, S(t) is the position of movable magnet measured from the equilibrium position, Se is the equilibrium position of the movable magnet, L is the length of the entire piezoelectric beam, d is the distance between tip of the cantilever and the fixed magnet and y(t) is the base excitation which is a function of time. The working principle of the system can also be explained by a variable potential function. The potential energy of the system is a double-well function when the distance between two magnets is below a threshold value, which is shown in Figure 3.

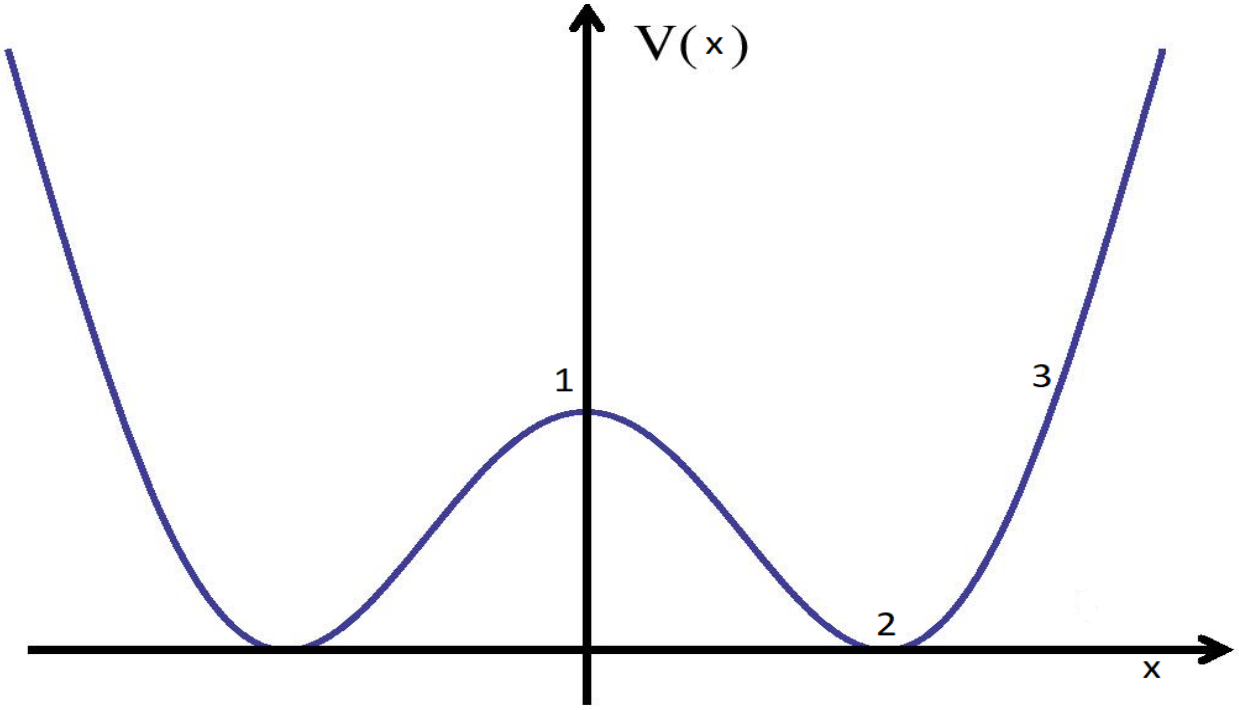

Figure 3: Double-well potential function

Consider a ball at position 1 compressing a spring that represents the beam in its initial position. As the ball moves down (as the beam vibrates), the spring releases the stored energy. The release of spring's energy helps the ball gain higher velocity at position 2 that pushes the ball to position 3, where the velocity of the ball slows to zero. At position 3, the ball has more potential energy than at the starting position (position 1) because of the added restoring energy of the spring.

Then the ball starts moving back. On the way back (from position 2 to position 1), the ball compresses the spring. In this variable potential concept, the key for increasing the height of the ball (equivalent to the beam amplitude) is therefore the added potential energy of the spring. This results in larger electrical energy output.

2.2 Governing equation

To analyze the dynamic response and output voltage of the energy harvester, a mathematical coupled model for the cantilever under the influence of magnets and also the piezoelectric strip is derived. The electromechanical model of the piezoelectric behavior is ruled by the subsequent constitutive laws relating the mechanical stress to the electrical field generated inside a layer

$$D_3 = \varepsilon_{33}^{S} E_z + e_{31} T_{1s}$$

$$S_1 = c_{11} T_{1s} + e_{31} E_z \qquad (1)$$

where D_3 is the electric displacement, ε_{33}^{S} is the piezoelectric material permittivity constant, E_z is the electric field, e_{31} is the piezoelectric constant, T_{1s} is the mechanical stress, S_1 is the mechanical strain and c_{11} is the compliance of piezoelectric. As we are considering parallel connection of piezoelectric layers, the electrical field (E_z) produced can be written with respect to flux linkage $\lambda(t)$ as

$$\mathrm{E_z} = -\frac{\dot{\lambda}(t)}{h_p} \qquad (2)$$

The electrical energy for one piezoelectric strip is given by $\frac{1}{2}\int E_z D_3 dv$, where v is the volume of piezoelectric strip. Therefore, the electrical energy of the system by considering two piezoelectric strips is

$$\int E_z D_3 dv = e_{31} b_p (h_p + h_s)\dot{\lambda}(t) w_x(L_p,t) + \varepsilon_{33}^s \frac{b_p L_p}{h_p}\dot{\lambda}(t)^2 \quad (3)$$

where L_p, b_p, h_p are the length, width and thickness of the piezoelectric respectively and L, b, h_s are the length, width and thickness of the beam and $w(x,t)$ represents lateral deflection of the beam. First we find the total energy of the system and then by using Hamilton's Principle and variational calculus we find out the equations of motion. Our analysis is the extension of the work by Siddiqui et al. [22] who analyzed the dynamics of a cantilever beam with a moving mass. In our case we convert the moving mass to a moving magnet facing a stationary magnet and add the piezoelectric strip.

The total kinetic energy of the system is

$$\mathrm{T} = \frac{1}{2}\int_0^L \rho A(\dot{w}+\dot{y})^2 dx + \frac{1}{2} m[\dot{s}\sin\beta + (\dot{w}+\dot{y})]^2 + \frac{1}{2} m(\dot{s}\cos\beta)^2 \quad (4)$$

where ρ is the density of the piezoelectric beam, A is the crossectional area of piezoelectric beam, m is the mass of the movable magnet, s is the magnet and β is the slope angle of the beam deflection curve with the horizontal line assuming $\sin\beta = \frac{dw}{dx}$.

The total potential energy of the system including the electric energy is

$$\mathrm{V} = \frac{1}{2}\int_0^L EIw_{xx}^2 dx + \frac{1}{2} ks^2 + U_{mag} - \theta_e \dot{\lambda}(t) w_x(L_p,t) - \frac{1}{2} c_p \dot{\lambda}(t)^2 \quad (5)$$

where E is the modulus of elasticity, I is the moment of inertia, k is the stiffness of the spring, U_{mag} is the magnetic potential energy and

$$\theta_e = e_{31} b_p (h_p + h_s)$$

$$\mathrm{c_p} = \varepsilon_{33}^s \frac{2 b_p L_p}{h_p}$$

To obtain the governing equations of motion, the extended Hamilton's Principle,

$$\int_{t_1}^{t_2}[\delta(T-V)+I\delta\lambda]dt=0$$

is used where t_1 and t_2 are two different time instants in which the variation, δ is calculated. The variations are determined for kinetic energy (T), potential energy (V), and virtual work ($I\delta\lambda$) due to the developed current (I, ratio of change of flux linkage to the resistance load R), respectively that yields. So substituting equations (4), (5) into the extended Hamilton's Principle equation and simplifying we get

$$\int[\int-\rho A\ddot{w}dx\delta w-\int EIw_{xxxx}dx\delta w-EIw_{xx}\delta w_x\Big|_0^L+EIw_{xxx}\delta w\Big|_0^L+m\dot{s}\delta\dot{s}-ks\delta s-\delta U_{mag}$$

$$+m(\dot{w}+\dot{y})\delta\dot{w}+m\delta w_x(\dot{w}+\dot{y})\dot{s}+\theta_e\delta\dot{\lambda}(t)w_x(L_p,t)+c_p\dot{\lambda}(t)\delta\dot{\lambda}(t)-\frac{\dot{\lambda}(t)}{R}\delta\lambda(t)]dt=0 \qquad (6)$$

The boundary conditions of a cantilever beam are used as

$$\frac{\partial^3 w(x,t)}{\partial x^3}=0 \text{ at x = L}$$

$$\frac{\partial^2 w(x,t)}{\partial x^2}=0 \text{ at x = L} \qquad (7)$$

$$\frac{\partial w(x,t)}{\partial x}=0 \text{ at x = 0}$$

$$w(x,t)=0 \text{ at x = 0}$$

To obtain the ordinary differential equations from the partial differential equations, Galerkin's method with a trial function of the form

$$\text{w(x,t)} = \sum_{i=1}^{n}\phi_i(x)\alpha_i(t)$$

is used, where $\phi_i(x)$ is the mode shape of the cantilever beam, i indicates the mode shape number and $\alpha_i(t)$ is the dynamic response of the cantilever beam. We take only the first mode shape of the cantilever (i = 1) to reduce the complexity of derivation. The normalized first mode shape is given by

$$\phi_1(x) = \cosh(k_1 x) - \cos(k_1 x) - \frac{\cos(k_1) + \cosh(k_1)}{\sin(k_1) + \sinh(k_1)}(\sinh(k_1 x) - \sin(k_1 x))$$

where k_1 is the normalized first natural frequency of cantilever beam. Therefore, we have $\delta w = \phi(x)\alpha(t)$ and $\delta w_x = \phi'(x)\alpha(t)$. Integrating every term in equation (6) and using the boundary conditions, we obtain

$$\int [\phi(\int -\rho A \ddot{w} - EIw_{xxxx}\, dx)\delta\alpha - m\ddot{s}\delta s - ks\delta s + \phi F_{magx}\delta s + m(\dot{w} + \dot{y})\delta\dot{w} + mw_x\delta(\dot{w} + \dot{y})\dot{s}$$

$$+ \theta_e \delta w_x(L_p, t)\dot{\lambda}(t) + c_p\dot{\lambda}\delta\dot{\lambda}(t) - \frac{\dot{\lambda}(t)}{R}\delta\lambda(t)]dt = 0 \qquad (8)$$

where F_{magx} and F_{magy} are the magnetic force tangential and normal to the beam directions respectively and

$$\int m(\dot{w} + \dot{y})\delta\dot{w}\,dt = \int(-m\phi(\ddot{w} + \ddot{y})\delta\alpha - m\phi\dot{w}_x\dot{s}\delta\alpha)dt$$

$$\int mw_x\delta(\dot{w} + \dot{y})\dot{s}\,dt = \int(mw_x\dot{s}\delta\dot{w} + mw_x(\dot{w} + \dot{y})\delta\dot{s}\,dt) = \int(-m\phi w_x\ddot{s}\delta\alpha - m\phi\dot{w}_x\dot{s}\delta\alpha$$
$$- m\phi w_{xx}\dot{s}^2\delta\alpha - mw_x(\ddot{w} + \ddot{y})\delta s)dt$$

$$\int[\theta_e \delta w_x(L_p,t)\dot{\lambda}(t) + c_p\,\dot{\lambda}(t)\delta\dot{\lambda}(t) - \frac{\dot{\lambda}(t)}{R}\delta\lambda(t)]dt = \int[-\theta_e\,\dot{w}_x(L_p,t)\delta\lambda(t) + \theta_e\phi'(L_p)\,\dot{\lambda}(t)\delta\alpha$$

$$- c_p\,\dddot{\lambda}(t)\delta\lambda(t) - \frac{\dot{\lambda}(t)}{R}\delta\lambda(t)]dt$$

Then the coefficients of δs, $\delta\alpha$ and $\delta\lambda(t)$ in equation (8) are set to be zero respectively which gives us three coupled differential equations as

$$m\ddot{s}(t) + ks(t) + mw_x(x,t)\ddot{w}(x,t) + mw_x(x,t)\ddot{y}(t) - F_{magx} = 0 \tag{9}$$

$$\phi\left(\int_0^L \rho A\ddot{w}(x,t) + EIw_{xxxx}(x,t)dx\right) + m\phi f_a + \phi\int_0^L \rho A dx\,\ddot{y}(t) + m\phi\,\ddot{y}(t) - \phi F_{magy} - \theta\dot{\lambda}(t) = 0 \tag{10}$$

$$c_p\,\ddot{\lambda}(t) + \theta_e\,\dot{w}_x(L_p,t) + \frac{\dot{\lambda}(t)}{R} = 0 \tag{11}$$

where the coupled acceleration term for the mass is

$$f_a = \ddot{w} + 2\dot{w}_x\dot{s} + w_{xx}\dot{s}^2 + w_x\ddot{s}$$

Each term in the coupled acceleration represents different acceleration for the beam where the first term represents the acceleration of the beam in the horizontal direction, second is the Coriolis acceleration, third is centripetal acceleration and the fourth term is the acceleration of the mass projected in the horizontal direction. We follow the assumption that the beam is allowed to undergo small oscillation around equilibrium caused by small excitation and that nonlinearity from strain displacement is also not included in the governing equations.

Table 1: Energy harvester parameters used in simulation

Parameter	Value
Mass of moving magnet, m	4 g
Magnet size	8 mm × 8 mm × 8 mm
Mass of beam	5.6 g
Length of beam, L	75 mm
Width of beam, b	10 mm
Thickness of beam, h_s	1 mm
Flexural rigidity, EI	0.003 Pa. m^4
Damping ratio, μ_1 and μ_2	0.1
Stiffness of the spring, k	250 N/m
Original length of the spring, s_0	57.75 mm
Distance between the beam tip and fixed magnet, d	4.5 mm
Magnetization moment, N	0.53 A m^2
Length of piezoelectric, L_p	75 mm
Width of piezoelectric, b_p	10 mm
Thickness of piezoelectric, h_p	0.254 mm
Permittivity of free space, ε_0	8.854×10^{-12} F/m
Laminate permittivity, ε_{33}	$3200\,\varepsilon_0$
Coupling coefficient, ε_{31}	-20
Equivalent resistive load, R	500 Ω

The magnetic force terms are

$$F_{magx} = \frac{F_R}{D^4}\left(1 - \frac{5w^2}{2D^2}\right)$$

$$F_{magy} = \frac{F_R w}{D^5}\left(1 - \frac{5w^2}{2D^2}\right), \quad \text{where } F_R = \frac{3\mu_0 N^2}{2\pi} \text{ and } D = D(t) = L + d - s(t)$$

In the above equation F_R is the resultant magnetic force, N is the magnetization moment of the magnet, μ_0 is the permeability of space and D is the horizontal distance between two magnets. The electromechanical coupling term is

$$\theta = \theta_e \phi'(L)$$

The static equilibrium equation is obtained by setting the time derivative terms equal to zero in equation (9)

$$\omega_s^2 (s_0 - s_e) - \frac{F_R}{mD^4} = 0 \tag{12}$$

where ω_s is the natural frequency of the spring and s_0 is the original length of the spring. Assuming parameters of the system as listed in Table 1, equation (12) is solved to obtain the static equilibrium position (s_e). To further simplify the equations, the governing equations (9) and (10) are expanded about their equilibrium points. An Taylor series expansion is used about the equilibrium position and terms up to the first derivatives are only included which gives

$$\frac{1}{D^n} = \frac{1}{D_e^n} + \frac{nS}{D_e^{n+1}}$$

$$\phi(x)_{x=s(t)} = \phi_e + \phi_e' S$$

where $S = S(t) = s(t) - s_e$ is the dynamic response of the movable magnet about the equilibrium point. $D_e = L + d - s_e$ and $\phi_e = \phi(s_e)$, $\phi_e' = \phi'(s_e)$. The mode shape of the cantilever is

expanded using Taylor series around the equilibrium position of the movable magnet and is substituted into governing equations (9) and (10). Neglecting static terms gives

$$\ddot{S}+\omega_s^2 S+\phi_e\phi_e^{'}\ddot{\alpha}\alpha+\alpha\phi_e^{'}\ddot{y}-\frac{F_R}{mD^4}\left\{\frac{4S}{D_e}+\frac{-5}{2}\left(\frac{1}{D_e^2}+\frac{6S}{D_e^3}\right)\alpha^2(\phi_e+\phi_e^{'}(s))^2\right\}=0 \tag{13}$$

$$\begin{aligned}&\int_0^L EI\phi^{''2}dx\,\alpha+\int_0^L \rho A\phi^2 dx\,\ddot{\alpha}+(\phi_e+\phi_e^{'}(s))\left(\int_0^L \rho A dx+m\right)\ddot{y}+m\phi_e^2\ddot{\alpha}+2mS\phi_e\phi_e^{'}\ddot{\alpha}+m\phi_e\phi_e^{'}\ddot{S}\alpha+2m\phi_e\phi_e^{'}\dot{S}\dot{\alpha}\\&+m\dot{S}^2\alpha\phi_e\phi_e^{''}+mS^2\ddot{\alpha}\phi_e^{'2}-\theta\dot{\lambda}(t)-\frac{F_R\alpha(\phi_e+\phi_e^{'}S)^2}{D_e{}^5}\left\{\left(1+\frac{5S}{D_e}\right)+\frac{-5}{2}\left(\frac{1}{D_e^2}+\frac{7S}{D_e^3}\right)\alpha^2(\phi_e+\phi_e^{'})^2\right\}=0\end{aligned} \tag{14}$$

where

$$\int_0^L EI\phi^{''2}dx=\int_0^L EI\phi\phi^{''''}dx$$

Nonlinear terms with orders higher than quadratic in equations (13) and (14) are neglected. For the vibration of the beam, introducing air viscous damping we add two damping terms μ_n which gives

$$\ddot{S}+\omega^2 S+2\mu_1\dot{S}+c_1\ddot{\alpha}\alpha+c_2\alpha^2+\phi^{'}\alpha\ddot{y}=0 \tag{15}$$

$$\ddot{\alpha}+\omega_1^2\alpha+2\mu_2\dot{\alpha}+2mc_4\dot{S}\alpha+\dot{2}mc_4 S\dot{\alpha}+mc_4\ddot{S}\alpha+c_5 S\alpha-\theta\dot{\lambda}(t)+(\phi_e+\phi_e^{'}S)c_y\ddot{y}=0 \tag{16}$$

$$c_p\ddot{\lambda}(t)+\theta\dot{\alpha}+\frac{\dot{\lambda}(t)}{R}=0 \tag{17}$$

where

$$\omega^2=\omega_s^2+c_3 \tag{18}$$

$$c_1=\phi_e\phi_e^{'} \tag{19}$$

$$c_2 = \frac{5F_R\phi_e^2}{2mD_e^6} \tag{20}$$

$$c_3 = -\frac{4F_R}{mD_e^5} \tag{21}$$

$$\omega_1^2 = \frac{\int_0^L EI\phi''^2 dx}{\int_0^L \rho A\phi^2 dx + m\phi_e^2} - \frac{F_R\phi_e^2}{\left(\int_0^L \rho A\phi^2 dx + m\phi_e^2\right)D_e^5} \tag{22}$$

$$c_4 = \frac{\phi_e\phi_e'}{\int_0^L \rho A\phi^2 dx + m\phi_e^2} \tag{23}$$

$$c_5 = -\frac{F_R}{\int_0^L \rho A\phi^2 dx + m\phi_e^2}\left(\frac{2\phi_e\phi_e'}{D_e^5} + \frac{5\phi_e^2}{D_e^6}\right) \tag{24}$$

$$c_y = \frac{\int_o^L \rho A dx + m}{\int_0^L \rho A\phi^2 dx + m\phi_e^2} \tag{25}$$

It is clear that the last term in equations (15) and (16) are parametric excitation terms. A parametric excitation has a zero steady-state response below certain initial threshold amplitude and therefore small non-zero initial displacement condition is required as shown by Y. Jia et al. [23]. Therefore, in our case, direct excitation is analyzed while neglecting the parametric excitation condition. The relationship between voltage *v(t)* and flux linkage $\lambda(t)$ is $v(t) = \dot{\lambda}(t)$. Considering only the direct excitation equations (15) - (17) becomes

$$\ddot{S} + \omega^2 S + 2\mu_1\dot{S} + c_1\ddot{\alpha}\alpha + c_2\alpha^2 = 0 \tag{26}$$

$$\ddot{\alpha} + \omega_1^2 \alpha + 2\mu_2 \dot{\alpha} + 2mc_4 \dot{S}\alpha + 2mc_4 S\dot{\alpha} + mc_4 \ddot{S}\alpha + c_5 S\alpha - \theta v(t) = F\cos(\Omega t + \tau) \quad (27)$$

$$c_p \dot{v}(t) + \theta\dot{\alpha} + \frac{v(t)}{R} = 0 \quad (28)$$

where $F\cos(\Omega t + \tau) = -\phi_e c_y \ddot{y}$

2.3 Method of multiple scales

The method of multiple scales is used to obtain an analytical solution to the governing equations and to study the effects on the response by changing different system parameters. Two time scales T_0 (fast) and T_1 (slow) are used.

$T_0 = t$

$T_1 = \varepsilon t$

where ε is a scaling parameter. Let F = ε f, the governing equations become

$$\ddot{S} + \omega^2 S + \varepsilon(2\mu_1 \dot{S} + c_1 \ddot{\alpha}\alpha + c_2\alpha^2) = 0 \quad (29)$$

$$\ddot{\alpha} + \omega_1^2 \alpha + \varepsilon(2\mu_2 \dot{\alpha} + 2mc_4 \dot{S}\alpha + 2mc_4 S\dot{\alpha} + mc_4 \ddot{S}\alpha + c_5 S\alpha - \theta v(t)) = \varepsilon f\cos(\Omega t + \tau) \quad (30)$$

$$c_p \dot{v}(t) + \theta\dot{\alpha} + \frac{v(t)}{R} = 0 \quad (31)$$

We assume an asymptotic series solution for $S(t)$, $\alpha(t)$ and $v(t)$. In this case, a two term expansion is assumed as

$$S(t) = S_1(T_0, T_1) + \varepsilon S_2(T_0, T_1)$$

$$\alpha(t) = u_1(T_0, T_1) + \varepsilon u_2(T_0, T_1) \quad (32)$$

$$v(t) = v_1(T_0, T_1) + \varepsilon v_2(T_0, T_1)$$

Neglecting second and higher order terms in order to simplify the derivation, time derivatives are written as

$$\frac{\partial}{\partial t} = \frac{\partial}{\partial T_0} + \varepsilon \frac{\partial}{\partial T_1}$$

$$\frac{\partial^2}{\partial t^2} = \frac{\partial^2}{\partial {T_0}^2} + 2\varepsilon \frac{\partial^2}{\partial T_0 \partial T_1}$$

Substituting the asymptotic series solution into the time derivatives gives

$$\dot{S} = \frac{\partial S_1}{\partial T_0} + \varepsilon \frac{\partial S_2}{\partial T_0} + \varepsilon \frac{\partial S_1}{\partial T_1} + \varepsilon^2 \frac{\partial S_2}{\partial T_1}$$

$$\ddot{S} = \frac{\partial^2 S_1}{\partial T_0^2} + \varepsilon \frac{\partial^2 S_2}{\partial T_0^2} + 2\varepsilon \frac{\partial^2 S_1}{\partial T_o \partial T_1} + 2\varepsilon^2 \frac{\partial^2 S_2}{\partial T_0 \partial T_1}$$

$$\dot{\alpha} = \frac{\partial u_1}{\partial T_0} + \varepsilon \frac{\partial u_2}{\partial T_0} + \varepsilon \frac{\partial u_1}{\partial T_1} + \varepsilon^2 \frac{\partial u_2}{\partial T_1}$$

$$\ddot{\alpha} = \frac{\partial^2 u_1}{\partial T_0^2} + \varepsilon \frac{\partial^2 u_2}{\partial T_0^2} + 2\varepsilon \frac{\partial^2 u_1}{\partial T_o \partial T_1} + 2\varepsilon^2 \frac{\partial^2 u_2}{\partial T_0 \partial T_1}$$

$$\dot{v} = \frac{\partial v_1}{\partial T_0} + \varepsilon \frac{\partial v_2}{\partial T_0} + \varepsilon \frac{\partial v_1}{\partial T_1} + \varepsilon^2 \frac{\partial v_2}{\partial T_1}$$

Putting the above equations into equations (29) - (31) and equating the coefficient of ε_0 and ε_1 to zero gives

ε^0 order:

$$\frac{\partial^2 S_1}{\partial T_0^2} + \omega^2 S_1 = 0 \tag{33}$$

$$\frac{\partial^2 u_1}{\partial T_0^2} + \omega^2 u_1 = 0 \tag{34}$$

$$c_p \frac{\partial v_1}{\partial T_0} + \frac{v_1}{R} = -\theta \frac{\partial u_1}{\partial T_0} \tag{35}$$

$\varepsilon^1 order$:

$$\frac{\partial^2 S_2}{\partial T_0^2} + \omega^2 S_2 = -2\mu_1 \frac{\partial S_1}{\partial T_0} - 2\frac{\partial^2 S_1}{\partial T_0 \partial T_1} - c_1 \frac{\partial^2 u_1}{\partial T_0^2} u_1 - c_2 u_1^2 \tag{36}$$

$$\frac{\partial^2 u_2}{\partial T_0^2} + \omega_1{}^2 u_2 = -2\mu_1 \frac{\partial u_1}{\partial T_0} - 2\frac{\partial^2 u_1}{\partial T_0 \partial T_1} - 2mc_4 \frac{\partial^2 u_1}{\partial T_0^2} S_1 - 2mc_4 \frac{\partial S_1}{\partial T_0}\frac{\partial u_1}{\partial T_0} - mc_4 \frac{\partial^2 S_1}{\partial T_0^2} u_1 - c_5 S_1 u_1 + f\cos(\Omega T_0 + \tau) + \theta v_1 \tag{37}$$

$$c_p \frac{\partial v_2}{\partial T_0} + \frac{v_2}{R} = -c_p \frac{\partial v_1}{\partial T_1} - \theta\left(\frac{\partial u_2}{\partial T_0} + \frac{\partial u_1}{\partial T_0}\right) \tag{38}$$

The solutions of equations (33) - (35) are given by

$$S_1 = P_1(T_1)e^{i\omega T_0} + \overline{P_1}(T_1)e^{-i\omega T_0} \tag{39}$$

$$u_1 =: P_2(T_1)e^{i\omega_1 T_0} + \overline{P_2}(T_1)e^{-i\omega_1 T_0} \tag{40}$$

$$v_1 = \frac{-i\omega_1 \theta P_2 e^{i\omega_1 T_0}}{\frac{1}{R} + i\omega_1 c_p} + \frac{i\omega_1 \theta \overline{P}_2 e^{-i\omega_1 T_0}}{\frac{1}{R} - i\omega_1 c_p} + E(T_1)e^{-\frac{T_0}{Rc_p}} \tag{41}$$

where P_1 and P_2 are complex variables and $E(T_1)$ is a variable. The overbars denote the complex conjugates. Substituting equations (39) - (41) into the right hand sides of equations (36) and (37) results in

$$rhs(36) = -2\mu_1 i\omega P_1 e^{i\omega T_0} + 2\mu_1 i\omega \overline{P_1} e^{-i\omega T_0} - 2i\omega \frac{\partial P_1}{\partial T_1} e^{-i\omega T_0} + 2i\omega \frac{\partial \overline{P_1}}{\partial T_1} e^{-i\omega T_0} + (c_1\omega_1^2 P_2 e^{i\omega_1 T_0} + c_1\omega_1^2 \overline{P_2} e^{-i\omega_1 T_0})(P_2 e^{i\omega_1 T_0} + \overline{P_2} e^{-i\omega_1 T_0}) - c_2 P_2^2 e^{2i\omega_1 T_0} - 2c_2 P_2 \overline{P_2} - c_2 \overline{P_2}{}^2 e^{-2i\omega_1 T_0} \tag{42}$$

$$
\begin{aligned}
rhs(37) = & -2\mu_2 i\omega_1 P_2 e^{i\omega T_0} + 2\mu_2 i\omega_1 \overline{P_2} e^{-i\omega T_0} - 2i\omega_1 \frac{\partial P_2}{\partial T_1} e^{i\omega_1 T_0} + 2i\omega_1 \frac{\partial \overline{P_2}}{\partial T_1} e^{-i\omega_1 T_0} \\
& + mc_4(2\omega_1^2 + \omega^2 + 2\omega\omega_1) P_1 P_2 e^{i(\omega_1+\omega)T_0} + mc_4(2\omega_1^2 + \omega^2 - 2\omega\omega_1)\overline{P}_1 P_2 e^{i(\omega_1-\omega)T_0} \\
& + mc_4(2\omega_1^2 + \omega^2 + 2\omega\omega_1)\overline{P}_1 \overline{P}_2 e^{-i(\omega_1+\omega)T_0} + mc_4(2\omega_1^2 + \omega^2 - 2\omega\omega_1) P_1 \overline{P}_2 e^{-i(\omega_1-\omega)T_0} \\
& - c_5(P_1 e^{i\omega T_0} + \overline{P}_1 e^{-i\omega_1 T_0})(P_2 e^{i\omega T_0} + \overline{P}_2 e^{-i\omega_1 T_0}) + \frac{1}{2} e^{i(\Omega T_0 + \tau)} + \frac{1}{2} e^{-i(\Omega T_0 + \tau)} \\
& + \theta \left(\frac{-i\omega_1 \theta P_2 e^{i\omega_1 T_0}}{\frac{1}{R} + i\omega_1 c_p} + \frac{i\omega_1 \theta \overline{P}_2 e^{-i\omega_1 T_0}}{\frac{1}{R} - i\omega_1 c_p} + E(T_1) e^{-\frac{T_0}{Rc_p}} \right)
\end{aligned}
\tag{43}
$$

To eliminate the secular terms, the coefficients of $e^{i\omega T_0}$ and $e^{i\omega_1 T_0}$ in equations (42) and (43) are set to zero. To study the solution for the coupled motion, we analyze the internal resonance case, assuming

$$\omega = 2\omega_1 + \varepsilon\sigma_2 \tag{44}$$

where σ_2 is small detuning parameter. When σ_2 is zero, we have internal resonance of 1:2 ratio (the ratio of the first frequency of the system to the frequency of the moving magnet). For the frequency of excitation (Ω) there are several cases. We consider the case when Ω is near to ω_1

$$\Omega = \omega_1 + \varepsilon\sigma_1 \tag{45}$$

where σ_1 is small detuning parameter. Applying the internal resonance relationship (44) and the condition (45), the elimination of secular terms no longer gives a linear solution. We have more nonlinear terms as

$$-2\mu_1 i\omega P_1 - 2i\omega \frac{\partial P_1}{\partial T_1} + c_1 \omega_1^2 P_2^2 e^{-i\sigma_2 T_1} - c_2 P_2^2 e^{-i\sigma_2 T_1} = 0 \tag{46}$$

$$-2\mu_2 i\omega_1 P_2 - 2i\omega_1 \frac{\partial P_2}{\partial T_1} + (2mc_4\omega_1^2 + mc_4\omega^2 - 2mc_4\omega\omega_1 - c_5)P_1\bar{P}_2 e^{i\sigma_2 T_1} + \frac{1}{2} fe^{i(\sigma T_1+\tau)}$$

$$+\left(\frac{-i\omega_1\theta^2 P_2}{\frac{1}{R}+i\omega_1 c_p}\right) \tag{47}$$

The complex variable P_1 and P_2 are described in polar form as

$$P_1(T_1) = \frac{1}{2} p_1(T_1) e^{i\varphi_1(T_1)}$$

$$P_2(T_1) = \frac{1}{2} p_2(T_1) e^{i\varphi_2(T_1)}$$

Setting the real and imaginary parts of equations (46) and (47) to zero respectively yields

$$\frac{\partial p_1}{\partial T_1} = -\mu_1 p_1 + \frac{a_{11}}{4\omega} p_2^2 \sin\gamma_1 \tag{48}$$

$$p_1 \frac{\partial \varphi_1}{\partial T_1} = -\frac{a_{11}}{4\omega} p_2^2 \cos\gamma_1$$

(49)

$$\frac{\partial p_2}{\partial T_1} = -\mu_2 p_2 - \frac{a_{22}}{4\omega_1} p_1 p_2 \sin\gamma_1 + \frac{f}{2\omega_1}\sin\gamma_2 + E_1 p_2 \tag{50}$$

$$p_2 \frac{\partial \varphi_2}{\partial T_1} = -\frac{a_{22}}{4\omega_1} p_1 p_2 \cos\gamma_1 - \frac{f}{2\omega_1}\cos\gamma_2 + E_2 p_2 \tag{51}$$

where

$$a_{11} = c_1\omega_1^2 - c_2$$

$$a_{22} = 2mc_4\omega_1^2 - 2mc_4\omega\omega_1 + mc_4\omega^2 - c_5$$

$$\gamma_1 = 2\varphi_2 - \varphi_1 - \sigma_2 T_1$$

$$\gamma_2 = \sigma_1 T_1 + \tau - \varphi_2$$

$$E_1 = -\frac{\frac{\theta^2}{2R}}{\frac{1}{R^2} + \omega_1^2 c_p^2}$$

$$E_2 = \frac{\frac{\theta^2 w_1 c_p}{2}}{\frac{1}{R^2} + \omega_1^2 c_p^2}$$

In equations (48) - (51) p_1 and p_2 are modal amplitudes and φ_1, φ_2 are corresponding phases.

For the steady-state response, we set $\frac{\partial p_1}{\partial T_1} = \frac{\partial p_2}{\partial T_1} = \frac{\partial \gamma_1}{\partial T_1} = \frac{\partial \gamma_2}{\partial T_1} = 0$ to obtain

$$\begin{aligned}&[a_{22}^2 \omega \sqrt{\mu_1^2 + (2\sigma_1 - \sigma_2)^2}\,] p_1^3 + [8 a_{22} \omega \omega_1 (\mu_1(\mu_2 - E_1) - (\sigma_1 - E_2)(2\sigma_1 - \sigma_2))] p_1^2 \\ &+ [16 \omega \omega_1^2 ((\mu_2 - E_1)^2 + (\sigma_1 - E_2)^2) \sqrt{\mu_1^2 + (2\sigma_1 - \sigma_2)^2}\,] p_1 - a_{11} f^2 = 0\end{aligned} \tag{52}$$

$$p_2^2 = [\frac{4\omega}{a_{11}} \sqrt{\mu_1^2 + (2\sigma_1 - \sigma_2)^2}\,] p_1 \tag{53}$$

Solving equations (52) and (53) gives the amplitude frequency response. The amplitude of output voltage is given by

$$v = \frac{\omega_1 \theta}{\sqrt{\frac{1}{R^2} + \omega_1^2 c_p^2}}\, p_2 \tag{54}$$

The stability of the steady-state response can be determined by examining the eigenvalues. If all the eigenvalues of a Jacobian matrix have negative real parts, the corresponding steady state response is stable. If not, the corresponding steady-state response is unstable.

Chapter 3

RESULTS AND DISCUSSION

3.1 Simulation results

By solving equations (52) - (54) and substituting the values of the parameters from the Table 1 the response of the energy harvester is obtained. The parameters are chosen in such a way to have symmetric internal resonance of 1:2 at ω_1 = 16 Hz and ω = 32 Hz. The default value of base excitation is set to 1 g. The corresponding frequency response is shown in Figure 4 and the output voltage frequency response is shown in Figure 5. Solid lines represent the stable solution and dashed line represents the unstable solution. There are two branches that are tilted to two opposite directions leading to a broad bandwidth frequency response with a jumping phenomenon observed from varying the frequency of excitation, Ω. The response of the beam correlates to the voltage production of a piezoelectric strip as shown in Figure 5. As it can be deduced from these figures, there is a region near the central frequency where the solution is unstable. Figure 6 and Figure 7 shows the vibration amplitudes of the beam and movable magnet respectively as functions of the excitation level for different detuning parameters σ_1 respectively. A smaller σ_1 implies that the system works near the resonant frequency. On the contrary, a large value of σ_1 indicates that the system works far from the resonant frequency. There are two regimes for single and multiple solutions depending on the excitation level. In the multiple solution regions, two solutions are stable and one is unstable based on the sign of the eigenvalues.

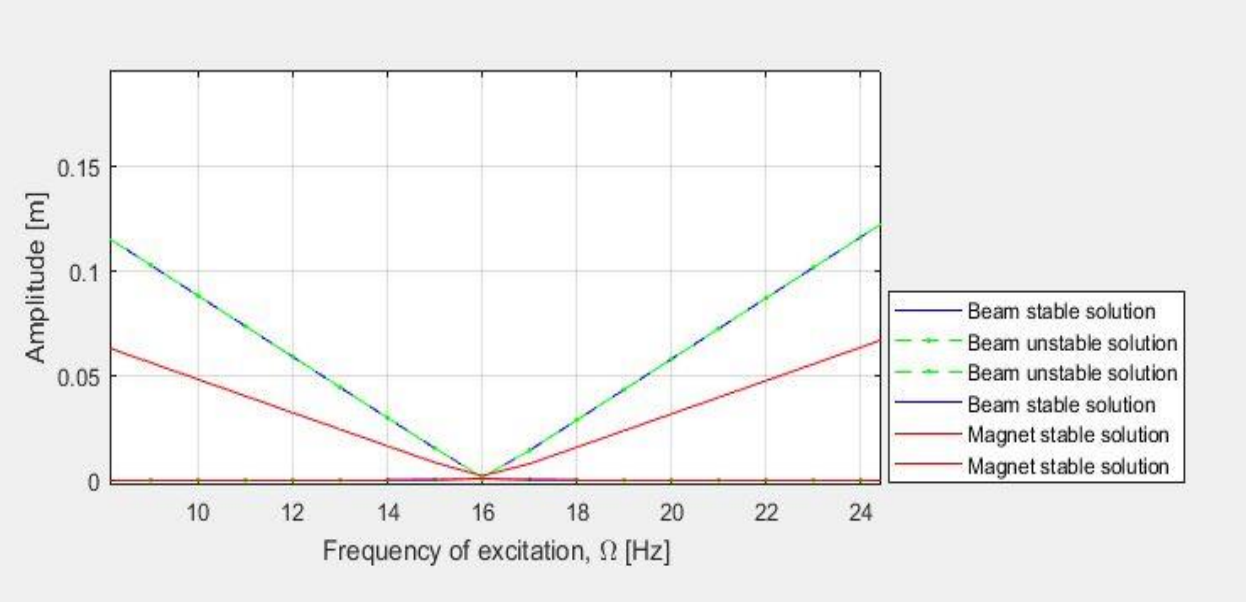

Figure 4: Frequency response for the beam and moving magnet

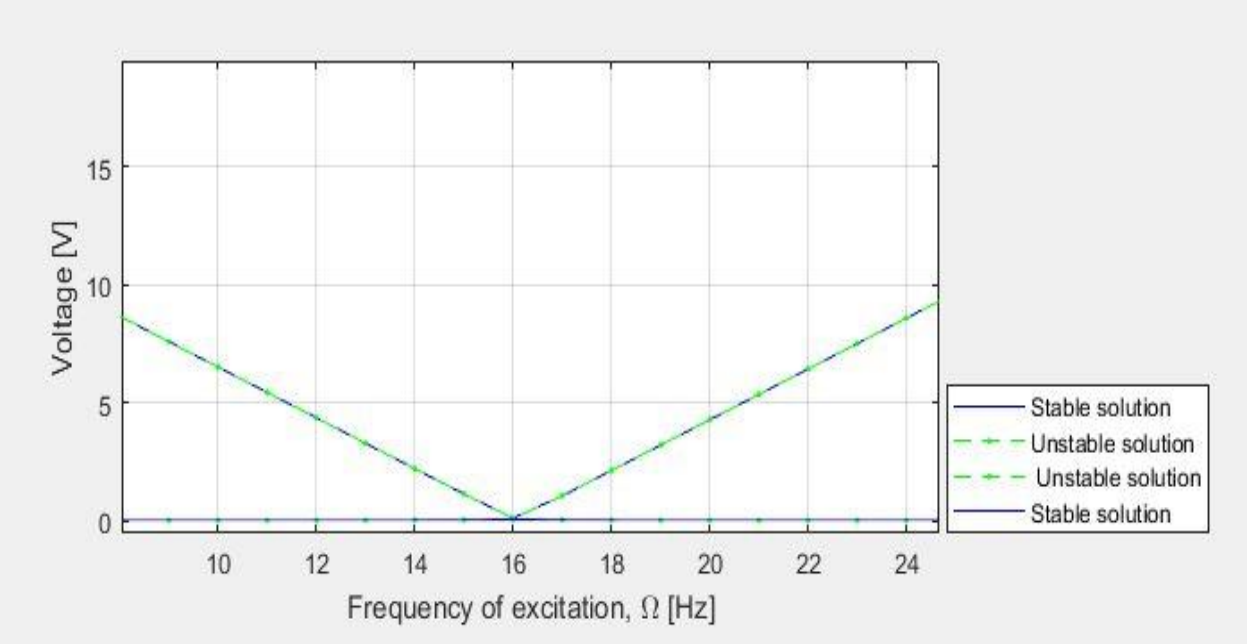

Figure 5: Output voltage frequency response

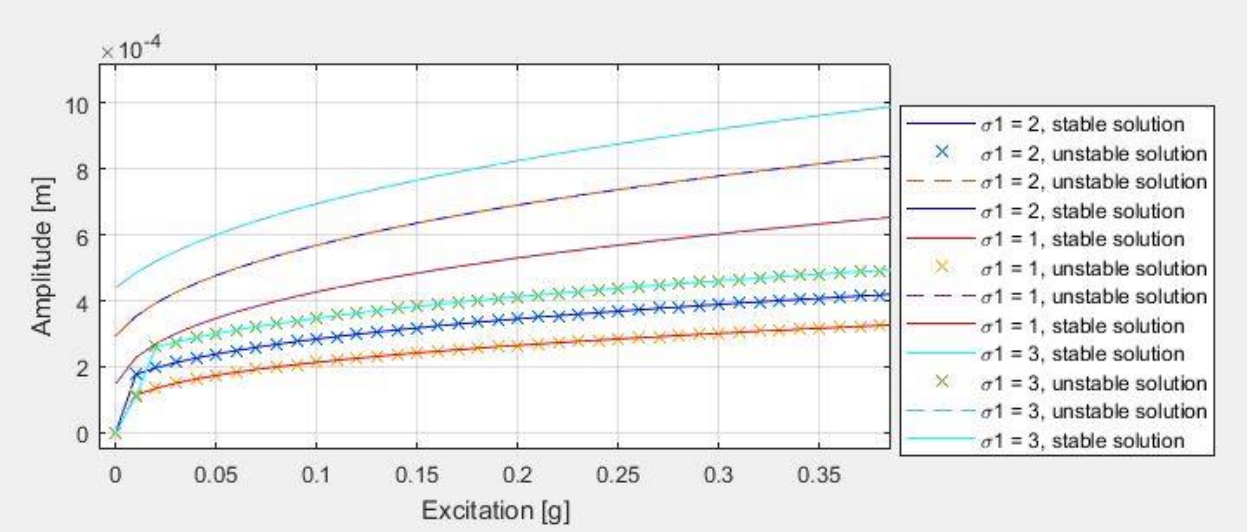

Figure 6: Beam vibration amplitude versus excitation level

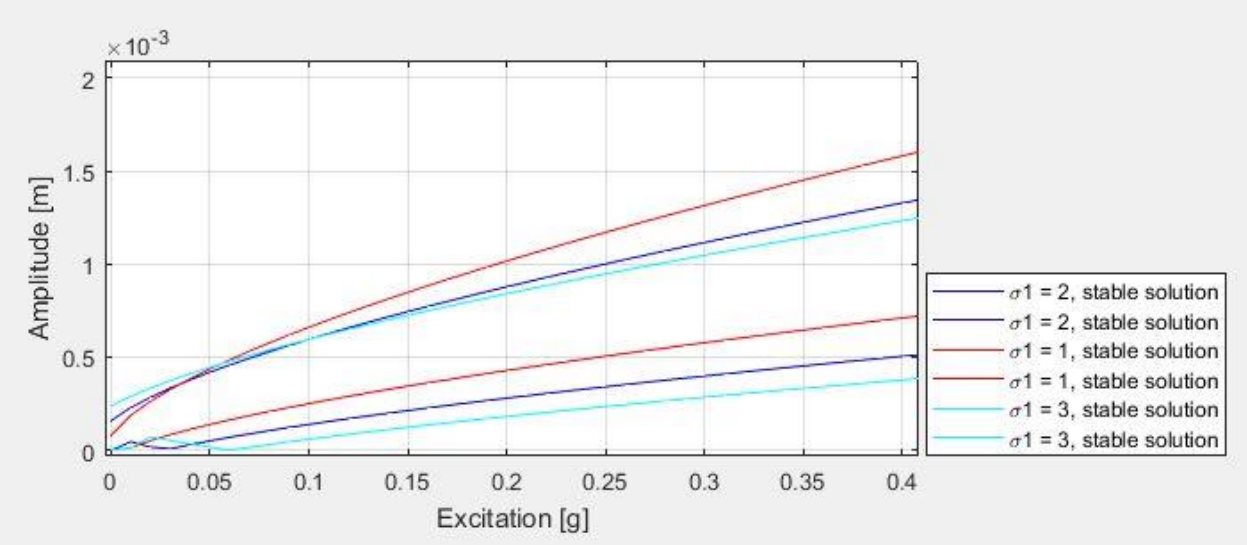

Figure 7: Moving magnet vibration amplitude versus excitation level

4.2 Parametric Study

This section studies the effects on energy harvesting by varying system parameters. Because the beam response affects the output voltage only the beam response and output voltage are analyzed. The displacement and voltage frequency responses are shown in Figures 8 and 9 for different levels of base excitation. The response amplitude, voltage and frequency bandwidth

increases with the excitation level. It is observed that the unstable frequency range in the middle increases with the excitation amplitude.

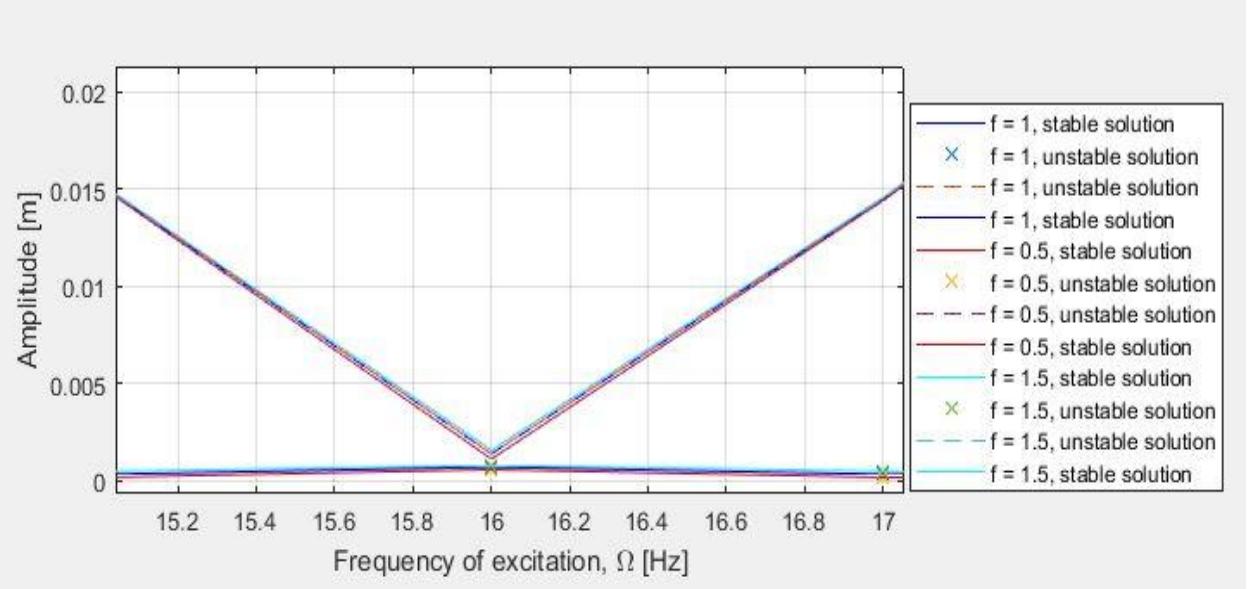

Figure 8: Frequency response for different excitation levels f(g)

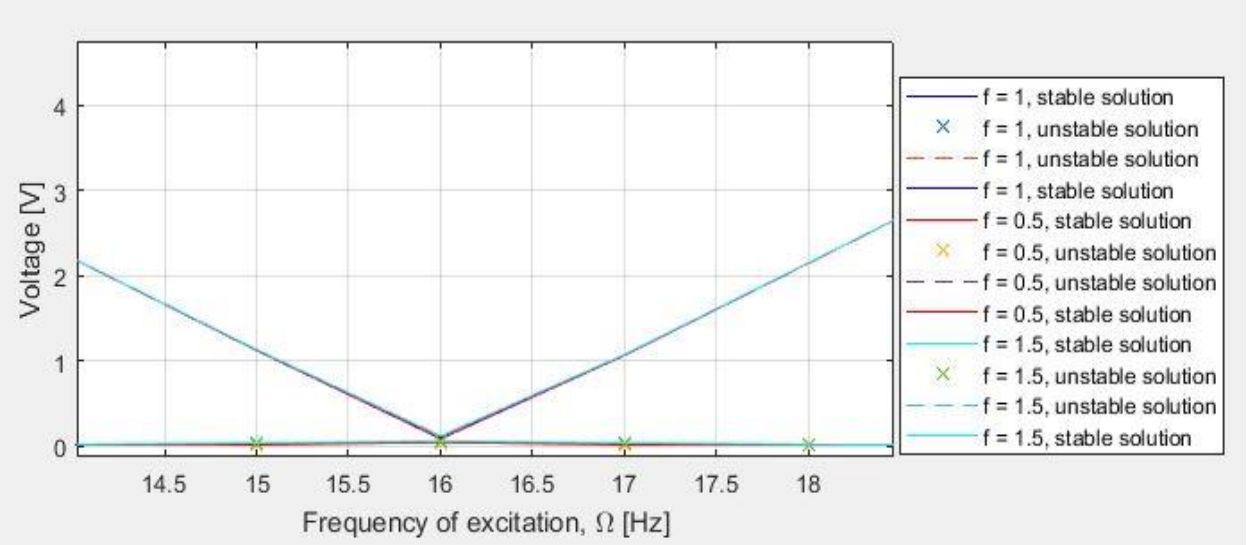

Figure 9: Output voltage for different excitation levels f(g)

The displacement and output voltage frequency responses for different stiffness values of spring '*k*' are shown in Figures 10 and 11. The value of spring stiffness 250 N/m results in symmetric internal resonance. Results show that as '*k*' decreases below 250 N/m, the central frequency of

the frequency response shifts to the left that is when $\sigma_2 < 0$ or $\omega < 2\omega_1$. Also the peak of right branch is larger than the left peak and will have a larger bandwidth on the right side of the central frequency. On the contrary, when '*k*' increases beyond 250 N/m, the behavior reverses. The stiffness of the spring breaks symmetry and changes the position of the central frequency with different performances on two branches.

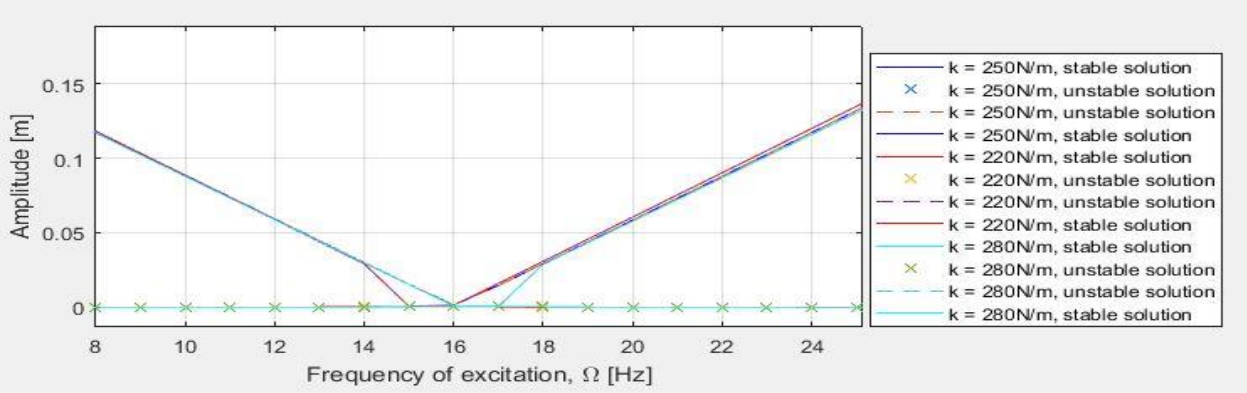

Figure 10: Frequency response for different spring stiffness '*k*' (N/m)

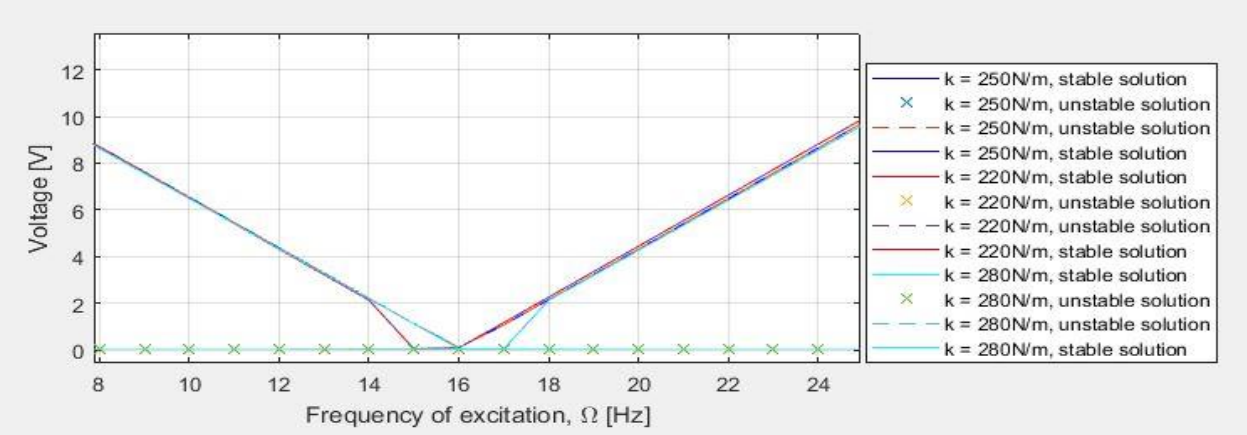

Figure 11: Output voltage for different spring stiffness '*k*' (N/m)

The initial distance between the beam tip and the fixed magnet, *d*, also affects the frequency responses as shown in Figures 12 and 13. Results show that when *d* decreases, a broader bandwidth response is obtained with a shift of the central frequency to the left compared to original curve. At smaller *d* values, the magnetic force is larger making a stronger bi-stability

effect that causes larger tilting in the frequency response and output voltage while maintaining large amplitude in the response.

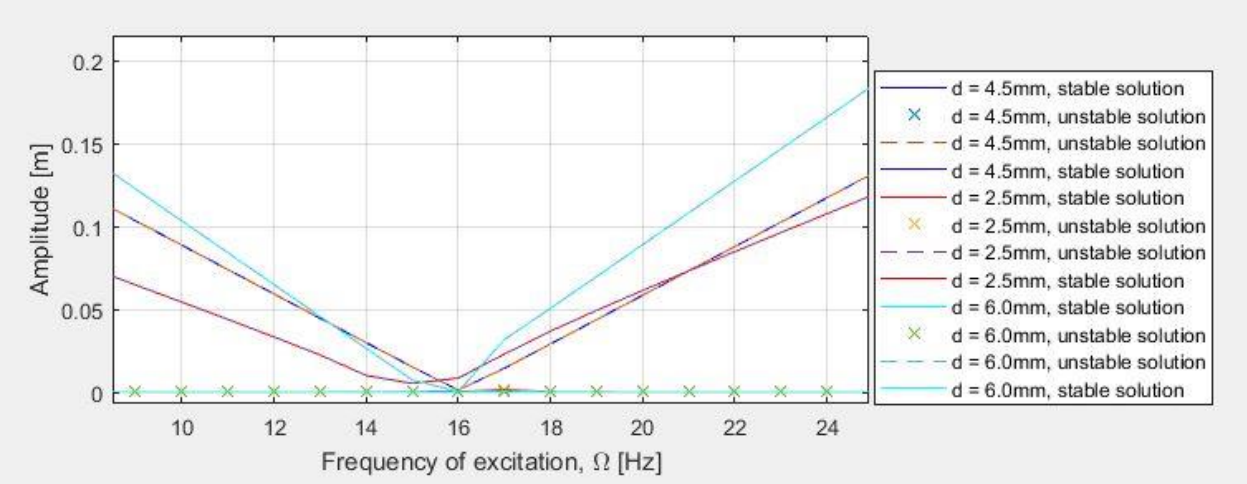

Figure 12: Frequency response for different distance‘*d*’ (mm)

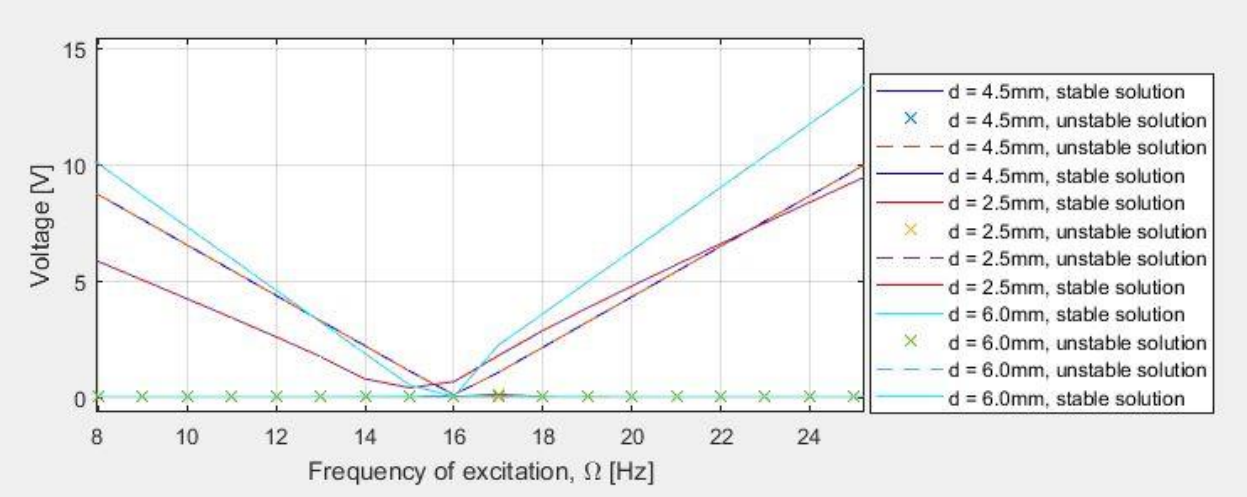

Figure 13: Output voltage for different distance‘*d*’ (mm)

The magnetization moment effect on the frequency responses is depicted in Figures 14 and 15. The effect is analogous to changing the distance between the tip of the cantilever and the fixed magnet (*d*). In both cases, as the magnetic force strengthens, more tilting occurs in the frequency response. The stronger nonlinear effect on the system creates a broader bandwidth frequency

spectrum. We also observe that increasing magnetization moment shifts the central frequency to the left.

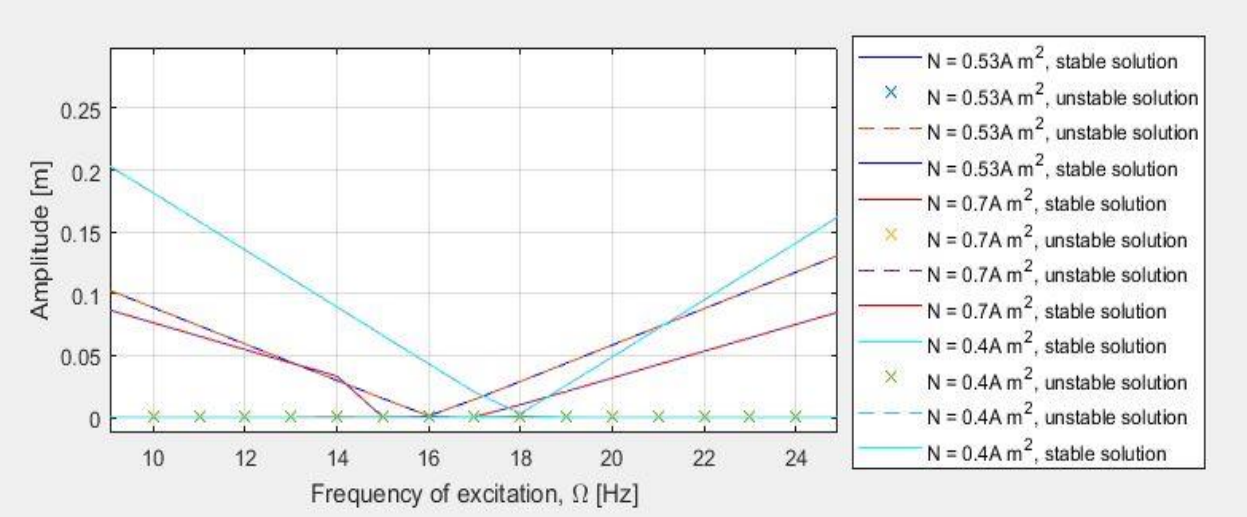

Figure 14: Frequency response for different magnetization moment '*N*' (A m^2)

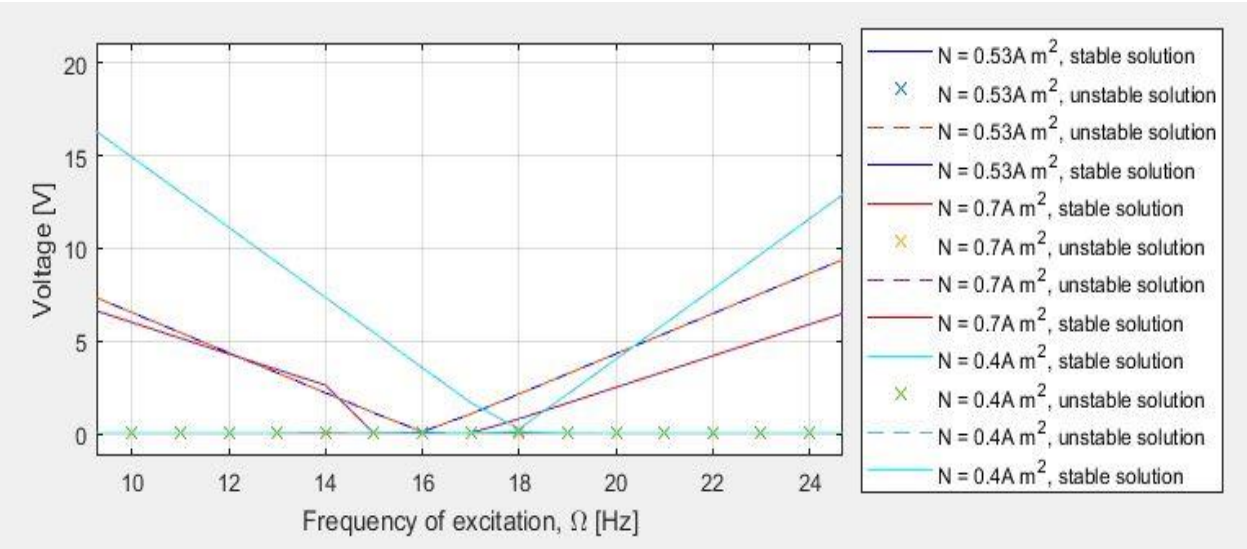

Figure 15: Output voltage for different magnetization moment '*N*' (A m^2)

Chapter 4

CONCLUSION

In this thesis, the dynamic behavior of a hybrid resonator that combines internal resonance with bi-stability is analyzed to enhance frequency bandwidth. The resonator consists of a piezoelectric cantilever beam carrying a movable magnet near the beams tip confronting a stationary magnet. The two magnets confront each other with the same pole to make a bi-stable framework, whereas internal resonance is created by adding a spring that controls the movable magnet. Three coupled governing equations are obtained by using Hamilton's energy approach. The perturbation method of multiple scales is used to get approximate analytical solutions for the amplitude and voltage frequency responses. The responses reveal a double bending effect where the two frequency peaks bend to opposite sides of the central frequency leading to a broader frequency bandwidth. The effects of various system parameters on the frequency response and output voltage are also analyzed. It can be seen that larger the magnetization moment and smaller the initial distance between magnets, larger the frequency bandwidth. Variation of spring stiffness changed the symmetry of the frequency response and shifted the central frequency; however, a large amplitude response was maintained. In summary, the hybrid energy harvester improves energy conversion efficiency by extending the frequency bandwidth of response and voltage combining the two effects of bi-stability and internal resonance.

BIBLIOGRAPHY

[1] Wei Yang, S.Towfighan, A hybrid nonlinear vibration energy harvester, Mechanical Systems and Signal Processing 90 (2017) 317–333.

[2] S.P. Pellegrini, N. Tolou, M. Schenk, J.L. Herder, Bistable vibration energy harvesters: a review, J. Intell. Mater. Syst. Struct. (2012), p.1045389X12444940.

[3] H. Liu, Y. Qian, N. Wang, C. Lee, An in-plane approximated nonlinear MEMS electromagnetic energy harvester, J. Microelectromech. Syst. 23 (3) (2014) 740–749.

[4] R. Masana, M.F. Daqaq, Relative performance of a vibratory energy harvester in mono-and bi-stable potentials, J. Sound Vib. 330 (24) (2011) 6036–6052.

[5] T. Yildirim, M.H. Ghayesh, W. Li, G. Alici, Design and development of a parametrically excited nonlinear energy harvester, Energy Convers. Manage. 126 (2016) 247–255.

[6] F. Cottone, H. Vocca, L. Gammaitoni, Nonlinear energy harvesting, Phys. Rev. Lett. 102 (8) (2009) 080601.

[7] B. Ando, S. Baglio, C. Trigona, N. Dumas, L. Latorre, P. Nouet, Nonlinear mechanism in MEMS devices for energy harvesting applications, J. Micromech. Microeng. 20 (12) (2010) 125020.

[8] B. Mann, N. Sims, Energy harvesting from the nonlinear oscillations of magnetic levitation, J. Sound Vib. 319 (1) (2009) 515–530.

[9] Y. Chen, T.E. Pollock, A. Salehian, Analysis of compliance effects on power generation of a nonlinear electromagnetic energy harvesting unit; theory and experiment, Smart Mater. Struct. 22 (9) (2013) 094027.

[10] D.A. Barton, S.G. Burrow, L.R. Clare, Energy harvesting from vibrations with a nonlinear oscillator, J. Vib. Acoust. 132 (2) (2010) 021009.

[11] M.F. Daqaq, Response of uni-modal duffing-type harvesters to random forced excitations, J. Sound Vib. 329 (18) (2010) 3621–3631.

[12] H.-X. Zou, W.-M. Zhang, K.-X. Wei, W.-B. Li, Z.-K. Peng, G. Meng, A compressive-mode wideband vibration energy harvester using a combination of bistable and flextensional mechanisms, J. Appl. Mech. 83 (12) (2016) 121005.

[13] H. Wu, L. Tang, Y. Yang, C.K. Soh, Development of a broadband nonlinear two-degree-of-freedom piezoelectric energy harvester, J. Intell. Mater. Syst. Struct. 25 (14) (2014) 1875–1889.

[14] L. Tang, Y. Yang, A nonlinear piezoelectric energy harvester with magnetic oscillator, Appl. Phys. Lett. 101 (9) (2012) 094102.

[15] B. Andò, S. Baglio, F. Maiorca, C. Trigona, Analysis of two dimensional, wide-band, bistable vibration energy harvester, Sens. Actuat. A: Phys. 202 (2013) 176–182.

[16] I. Sari, T. Balkan, H. Kulah, An electromagnetic micro power generator for wideband environmental vibrations, Sens. Actuat. A: Phys. 145 (2008) 405–413.

[17] A. Nayfeh, D. Mook, Nonlinear Oscillations, wiley, new york, 1979.

[18] C. Lan, W. Qin, W. Deng, Energy harvesting by dynamic unstability and internal resonance for piezoelectric beam, Appl. Phys. Lett. 107 (9) (2015) 093902.

[19] L.-Q. Chen, W.-A. Jiang, Internal resonance energy harvesting, J. Appl. Mech. 82 (3) (2015) 031004.

[20] D. Cao, S. Leadenham, A. Erturk, Internal resonance for nonlinear vibration energy harvesting, Eur. Phys. J. Special Top. 224 (14–15) (2015) 2867–2880.

[21] L.-Q. Chen, W.-A. Jiang, M. Panyam, M.F. Daqaq, A broadband internally resonant vibratory energy harvester, J. Vib. Acoust. 138 (6) (2016) 061007.

[22] S.A. Siddiqui, M.F. Golnaraghi, G.R. Heppler, Dynamics of a flexible cantilever beam carrying a moving mass, Nonlinear Dyn. 15 (2) (1998) 137–154.

[23] Y. Jia, A.A. Seshia, An auto-parametrically excited vibration energy harvester, Sens. Actuat. A: Phys. 220 (2014) 69–75.